

# RSC Advances



This is an *Accepted Manuscript*, which has been through the Royal Society of Chemistry peer review process and has been accepted for publication.

*Accepted Manuscripts* are published online shortly after acceptance, before technical editing, formatting and proof reading. Using this free service, authors can make their results available to the community, in citable form, before we publish the edited article. This *Accepted Manuscript* will be replaced by the edited, formatted and paginated article as soon as this is available.

You can find more information about *Accepted Manuscripts* in the [Information for Authors](#).

Please note that technical editing may introduce minor changes to the text and/or graphics, which may alter content. The journal's standard [Terms & Conditions](#) and the [Ethical guidelines](#) still apply. In no event shall the Royal Society of Chemistry be held responsible for any errors or omissions in this *Accepted Manuscript* or any consequences arising from the use of any information it contains.

# Selective removal of cationic dyes from aqueous solutions by an activated carbon-based multicarboxyl adsorbent

Libo Zhang<sup>1,2,3,4</sup>, Yuhang Liu<sup>1,2,3,4</sup>, Shixing Wang<sup>1,2,3,4\*</sup>, Bingguo Liu<sup>1,2,3,4</sup>, Jinhui Peng<sup>1,2,3,4</sup>

1 State Key Laboratory of Complex Nonferrous Metal Resources Clean Utilization, Kunming University of Science and Technology, Kunming 650093, China

2 National Local Joint Laboratory of Engineering Application of Microwave Energy and Equipment Technology, Kunming, Yunnan, 650093, China;

3 Key Laboratory of Unconventional Metallurgy, Ministry of Education, Kunming University of Science and Technology, Kunming, Yunnan 650093, China;

4 Faculty of Metallurgical and Energy Engineering, Kunming University of Science and Technology, Kunming 650093, China

## ABSTRACT

An activated carbon-based multicarboxyl adsorbent has been synthesized for selective removal of cationic dyes from aqueous solutions. The adsorbent was characterized by Fourier transform infrared spectroscopy (FT-IR), X-ray photoelectron spectroscopy (XPS), N<sub>2</sub> adsorption measurement and Zeta potential. The adsorption behavior of cationic rhodamine 6G on the activated carbon-based multicarboxyl adsorbent from aqueous medium was studied by varying the parameters such as pH, contact time and initial dye concentration. Dye adsorption was dramatically dependent of solution pH and the optimum pH is 4.45. After modified by multicarboxyl, the adsorption capacity of rhodamine 6G on the activated carbon dramatically increased from 33.18 mg/L to 122.55 mg/L at pH 4.45. The multicarboxyl adsorbent has obvious selectivity to cationic dyes. Adsorption isotherms could be well described by Langmuir model, adsorption kinetics fitted well with pseudo-second-order kinetic equation and exhibited 3-stage intraparticle diffusion mode. The electrostatic interaction was the main mechanism for the cationic dye adsorption.

**Keywords:** Activated carbon, multicarboxyl adsorbent, adsorption, Dye

## 1. Introduction

---

\* Corresponding author. Tel: +86 13529204964 E-mail: [wsxkm@sina.com](mailto:wsxkm@sina.com)

Dyes are gradually becoming one of the most hazardous materials in industrial effluents due to their damage to the human health<sup>1</sup> and the environmental life<sup>2</sup>. Many foundations industries (employed with textile, pulp mills, plastics and dyestuff manufacturing) use dyes to colorize products and consume plenty of water resource<sup>3</sup>, discharging highly colored wastewater. According to statistics, over 100,000 commercially available dyes exist and more than  $7 \times 10^5$  tons are produced annually<sup>4</sup>. What is worse, a variety of dyes are difficult to remove due to their stability and provoke serious environmental concerns all over the world<sup>5, 6</sup>. Therefore, reduction of dye concentration from effluents is required prior to handle. A new efficient method that can not only remove target toxic pollution but also achieve the possibility to reuse dyes in various industrial processing will be a promising application.

Over the past decades, many techniques employed for the removal of dyes have been researched<sup>7-12</sup>, including biological degradation, membrane separation, adsorption, ion exchange and flocculation. All these are based on the evaluation and comparison of many crucial parameters as cost, operation difficulty, handling period and effectiveness to toxic substances. The removal of organic pollutions from waters onto the various forms of AC is studied extensively in recent years. However, AC is a hydrophobic adsorbent which adsorbs non-polar or slightly polar substances and many researchers have reached the conclusion that it has a relatively low adsorption capacity for bulky dye molecules<sup>13-15</sup>. Therefore, AC is cost-ineffective for the treatment of wastewater with high level of dye contaminants. In general, the adsorption capacity enhance with the increase of adsorption active sites on the surface because the adsorption mainly takes place on the adsorbent surface<sup>16</sup>. So, AC are usually modified by a polymer matrix which introduces additional functional groups in order to improve the adsorption capacity and selectivity<sup>17</sup>. The AC modified by hexadecyltrimethylammonium had a higher adsorption capacity for Cr(VI) than that modified by cetylpyridinium<sup>18</sup>. Hameed et al. evaluated adsorptive capacities of a renewable waste tea activated carbon (WTAC) coalesced with chitosan for waste water treatment through batch and fixed-bed studies. They found that activated carbon-chitosan composite is a promising adsorbent for treatment of anionic and

cationic dyes in effluent wastewaters<sup>19</sup>. Mahmoud et al. designed activated carbon-immobilized-cationic surfactant to enhance the decolorization behavior of reactive black 5 from aqueous and industrial wastewater samples<sup>20</sup>. Recently, many researchers have proved the removal of dyes or heavy metals by grafting or introducing polymer matrix. Accordingly, how to develop AC with high adsorption capacity towards specific adsorbate remains a major concern.

In the presented work, the multicarboxyl adsorbent was prepared by grafting the multicarboxylic groups onto the AC modified by branch PEI. The multicarboxyl adsorbent has a high selectivity and capacity for cationic dyes. The multicarboxyl adsorbent was characterized by FT-IR, XPS, Zeta potential and N<sub>2</sub> adsorption-desorption measurement. Then, the adsorption performance of the multicarboxyl adsorbent for cationic dyes was investigated by varying the parameters such as contact time, pH and initial concentration. The adsorption isotherm and kinetic were systematically evaluated. Furthermore, the selective adsorption experiments were also carried out. Moreover, the primary mechanism for the dye adsorption on the multicarboxyl adsorbent was also studied.

## 2. Materials and methods

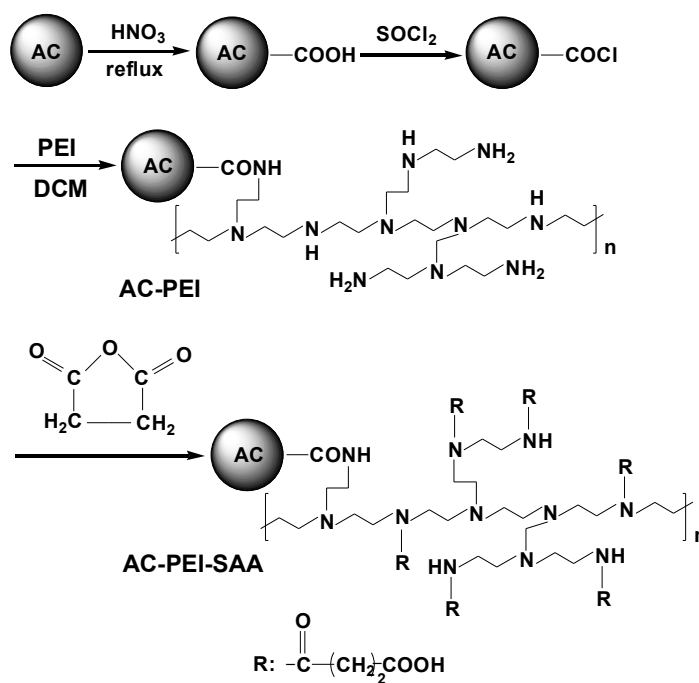
### 2.1. Materials

A granular activated carbon was purchased from Kelong Chemical Reagent Co., Ltd.(China). Branch polyethylenimine(PEI), succinate anhydride and five kinds of dyes were supplied by Aladdin Chemical Reagent Co., Ltd.(China). Thionyl chloride, triethylamine and anhydrous dichloromethane were obtained from Beijing NCS Analytical Instruments Co., (China). All chemicals were of analytical grade and used without further purification. Adjustment of pH was accomplished using 0.1M NaOH and 0.1M HCl.

### 2.2. Preparation of the multicarboxyl adsorbent

Activated carbon (10.0 g) was dispersed into 150 ml of concentrated HNO<sub>3</sub> (69 wt%) and the mixture was refluxed for 14 h. After oxidation, the oxidized AC (AC-COOH) was then centrifuged and filtered, washed with distilled water until

neutral pH and dried in oven. Secondly, 8.0 g of AC-COOH was allowed to react with 50 ml of thionyl chloride for 20 h and washed with anhydrous  $\text{CH}_2\text{Cl}_2$ , resulting in AC-COCl. The next step was to coat branch PEI on the AC-COCl. 6.5 g of AC-COCl and 2.0 g of branch PEI were dispersed in 80 ml of  $\text{CH}_2\text{Cl}_2$  at room temperature with magnetic stirring for 10 h. Subsequently the suspension was separated and washed with anhydrous dichloromethane, to obtain AC-PEI. Finally, 4.0 g of AC-PEI and 3.5 g succinate anhydride(SAA) were added to 150 ml of  $\text{CH}_2\text{Cl}_2$  in presence of triethylamine. The mixture was stirred at  $35^\circ\text{C}$  for 20 h. The resulting solid was washed and dried under vacuum, defined to AC-PEI-SAA. The modification process of AC with multicarboxyl is presented in **Scheme 1**.



Scheme 1. The functionalization process of AC with succinic anhydride

### 2.3. Characterization

Fourier transform infrared (FT-IR) spectra were recorded between 400 and 4000  $\text{cm}^{-1}$  using a Nicolet avatar 360 FT-IR spectrophotometer (Thermo Nicolet, USA) with a resolution of 4  $\text{cm}^{-1}$ . X-ray photoelectron spectroscopy (XPS) was performed on a PHI 5500 electron spectrometer (Physical Electronics, Inc., Chanhassen, MN, USA) using 200-W Mg radiations. The binding energies were referenced to the C1s line at 284.6 eV from adventitious carbon. Zeta potential measurements were

conducted using a ZetaPALS (Zeta Potential Analyzer using Phase Analysis Light Scattering, Brookhaven Instruments Corp, USA) with a voltage of 110-240V and frequency of 50-60 Hz. N<sub>2</sub> adsorption isotherm at 77 K were measured by using an automatic physical and chemical adsorption instrument (Aurosorb-1-C, Quantachrome, USA) to determine textural properties. The surface area was calculated using the BET (Brunauer, Emmett and Teller) equation from selected N<sub>2</sub> adsorption data within the range of relative pressure,  $p/p_0$ , from 0.1 to 0.3<sup>21</sup>. The concentration of dye in aqueous solution was measured by a UV spectrophotometer (UV-2401PC, Shimadzu, Japan).

#### 2.4 Batch adsorption

Batch adsorption experiments were conducted in a thermostated shaker with a shaking speed of 220 rpm using 10 ml centrifuge tubes with 20 mg AC-PEI-SAA. Adsorption isotherms were studied to describe the adsorption behavior and calculate adsorption capacity. 20 mg of AC-PEI-SAA were added into 10 ml rhodamine 6G (Rh6G) of different initial concentrations (120 mg/L-400 mg/L), the concentration of dyes left in the supernatant solution were measured by a UV-Vis spectrophotometer.

The amount of dye adsorbed onto AC-PEI-SAA was calculated from the mass balance equation as <sup>22</sup>:

$$q_e = \frac{(C_0 - C_e)V}{M} \quad (1)$$

where  $C_0$  and  $C_e$  are the initial and equilibrium concentrations (mg/L), while  $M$  and  $V$  are the weight of the adsorbent (g) and the volume of the solution (L), respectively.

Batch kinetic experiments were carried out by mixing 20 mg of AC-PEI-SAA to 10 ml of Rh6G solution with a known initial concentration (160 mg/L) and agitated in a thermostatic shaker at 25°C. The contact time was varied from 10 to 180 min resulting overall 13 samples. The concentration of Rh6G left in the supernatant solution was analyzed as above. Above each set of experiments was repeated three times and the average value was taken.

### 3. Results and discussions

## 3.1. Characterization of the adsorbent

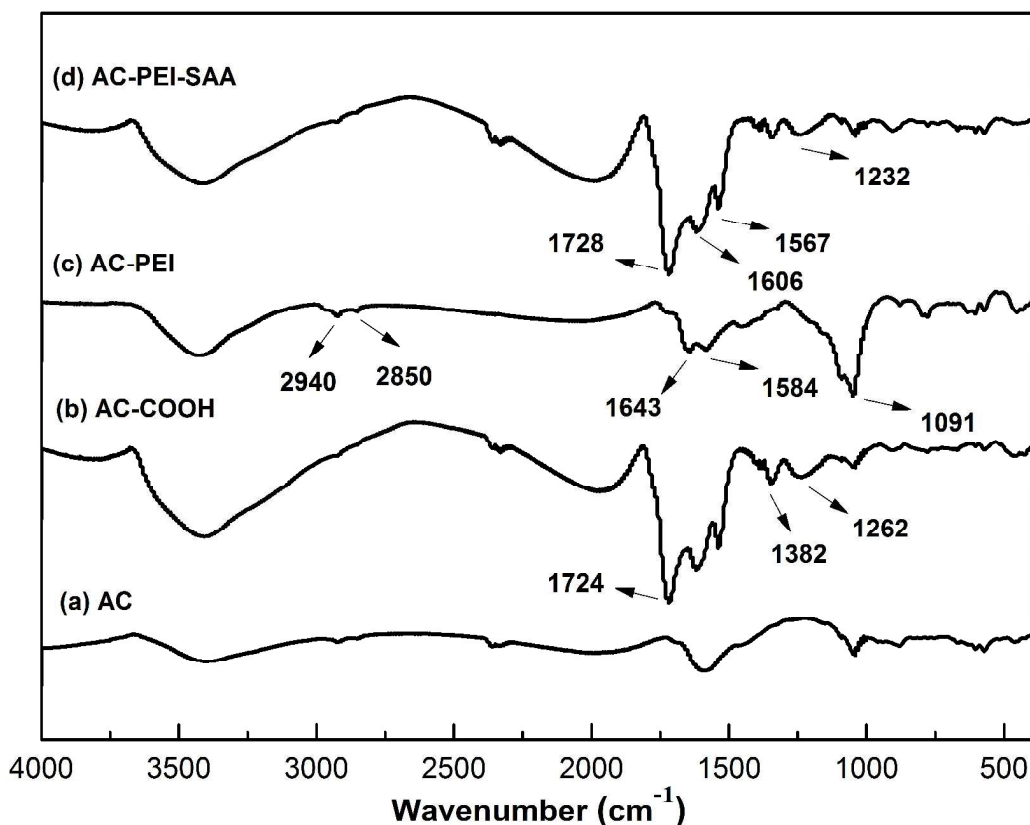


Fig. 1. FTIR spectra of AC(a), AC-COOH(b), AC-PEI(c) and AC-PEI-SAA(d)

The structure of AC-PEI-SAA was firstly identified by using FTIR spectrometry.

**Fig. 1** illustrates the FTIR spectra of pure AC, AC-COOH, AC-PEI and AC-PEI-SAA. In **Fig. 1b**, the absorbance at 3418, 1724, 1382, and 1262  $\text{cm}^{-1}$  are associated with AC after oxidation. The strong adsorption peaks at 3418  $\text{cm}^{-1}$  and 1724  $\text{cm}^{-1}$  are due to the stretching of hydroxyl groups from carboxylic acids<sup>23</sup> and the carboxyl (C=O) stretching vibration of the carboxylic acid, respectively. The C-O stretching and OH bending bands of carboxylic acids appear near 1320-1210  $\text{cm}^{-1}$  and 1440-1385  $\text{cm}^{-1}$ , respectively<sup>24</sup>. **Fig. 1c** is the FTIR spectra of AC-PEI. The characteristic peaks of PEI at 3350  $\text{cm}^{-1}$  (-N-H stretch of secondary amide), 2940 and 2850  $\text{cm}^{-1}$  (-C-H stretch), and 1091  $\text{cm}^{-1}$  (-C-N stretch)<sup>25</sup> can be seen. The peaks observed around 1643 and 1584  $\text{cm}^{-1}$  are attributed to secondary amide I and II band of -CONH-, which indicated that PEI was successfully grafted<sup>26</sup>. As depicted in **Fig. 1d**, the absorbances

at 1728 and 1567  $\text{cm}^{-1}$  provide the evidence of succinylation. The band at 1728  $\text{cm}^{-1}$  is the representative spectra of carbonyl group in carboxyl and esters, the band at 1567  $\text{cm}^{-1}$  corresponds to the asymmetric stretching of carboxylic anions<sup>27</sup>. Moreover, the intensity of the absorption band at 1606 and 1232  $\text{cm}^{-1}$  for C-O asymmetric stretching in ester groups increase after succinylation, which suggests the successful conjugation of SAA to AC-PEI<sup>28</sup>.

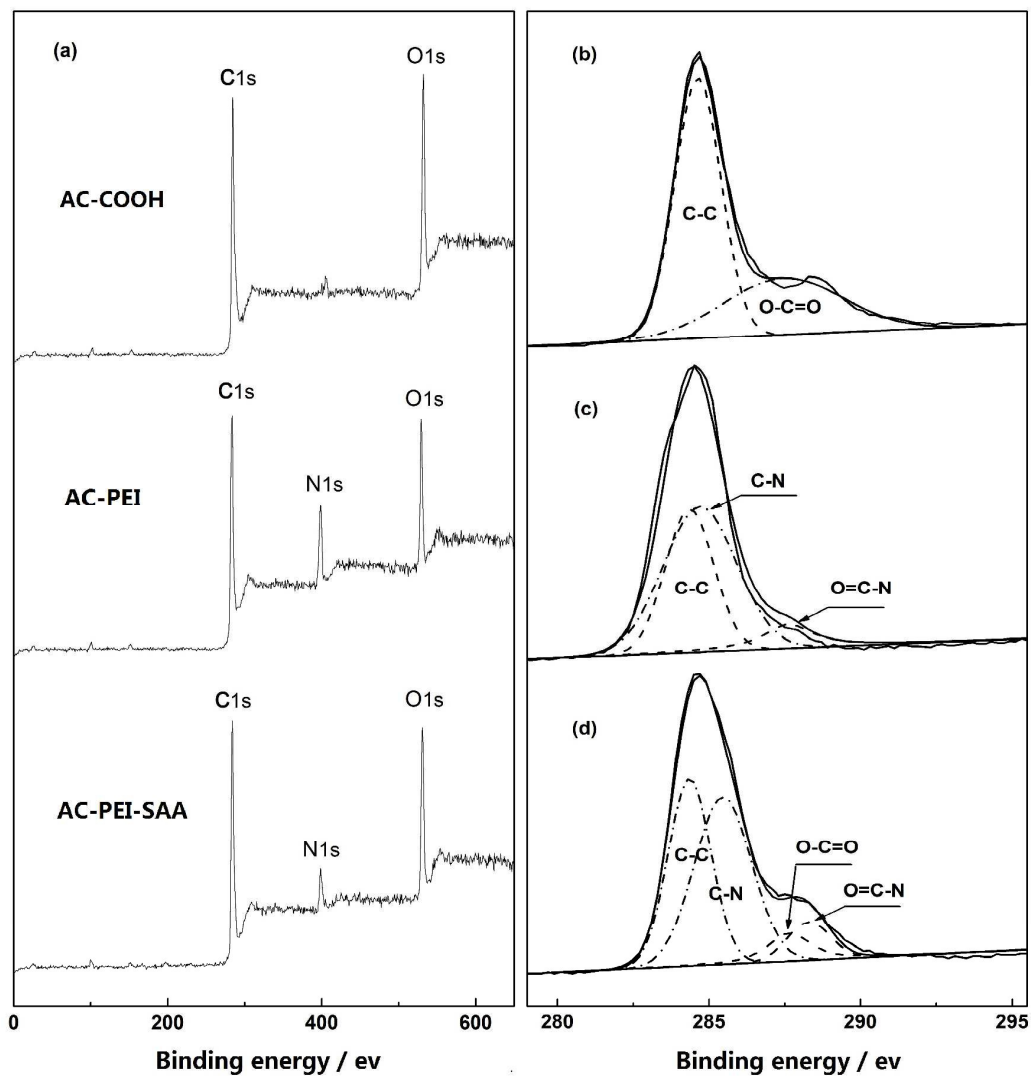


Fig. 2. XPS wide scans of AC-COOH, AC-PEI and AC-PEI-SAA(a), C1s of AC-COOH(b), AC-PEI(c) and AC-PEI-SAA(d)

X-ray photoelectron spectroscopy (XPS) was performed to further investigate the surface chemical composition and electronic structure of material surface. **Fig. 2a** presents the XPS survey spectra of AC-COOH, AC-PEI and AC-PEI-SAA samples. The XPS survey spectra of AC-COOH presented C1s and O1s. The peak intensity of

C1s in AC-PEI is higher than that of O1s. The XPS survey spectra of AC-PEI appeared N1s at the same time. The C1s signal at a binding energy of 284 eV, N1s signal at 400 eV and O1s signal at 531 eV are consistent with the presence of AC-PEI-SAA, the decreasing percentage of N1s in AC-PEI-SAA can be interpreted as the introduction of carboxyl. C1s deconvolution spectrums of above three samples are shown in **Fig. 2b-d**. The C1s of AC-COOH (**Fig. 2b**) can be further divided into two different peaks at 284.6 and 288.0 eV, attributed to the C-C and O-C=O species, respectively. For AC-PEI, two new peaks at 285, 288.2 eV are observed, corresponding to C-N and O=C-N groups, respectively (**Fig. 2c**). Furthermore, **Fig. 2d** shows that the C1s of AC-PEI-SAA consisted of four peaks at 284.6, 285, 288.0 and 288.2 eV, attributed to C-C, C-N, O-C=O, O=C-N groups. The results of XPS prove the successful synthesis of AC-PEI-SAA.

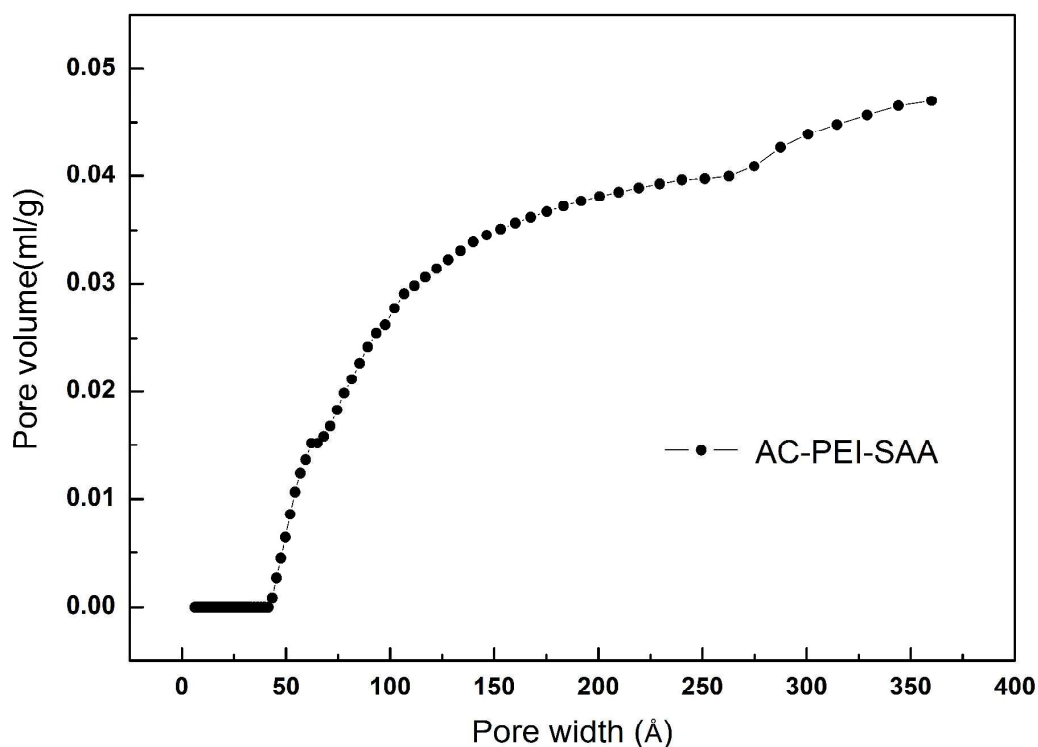


Fig. 3. The relationship between pore volume and pore width for AC-PEI-SAA.

Fig.3 shows the relationship between pore volume and pore width for AC-PEI-SAA. It is observed that there are no existence of micropores from 0 to 20 Å, indicating that materials may be mainly composed of mesopores and even macropores.

The surface area, pore volume and pore diameter of AC-PEI-SAA are  $15.31 \text{ m}^2/\text{g}$ ,  $0.067 \text{ cm}^3/\text{g}$  and  $30.42 \text{ nm}$ , respectively. These results further confirm that the grafted SAA was successfully located into the surface and changed the internal pore structure of material.

### 3.2 Effect of pH on adsorption

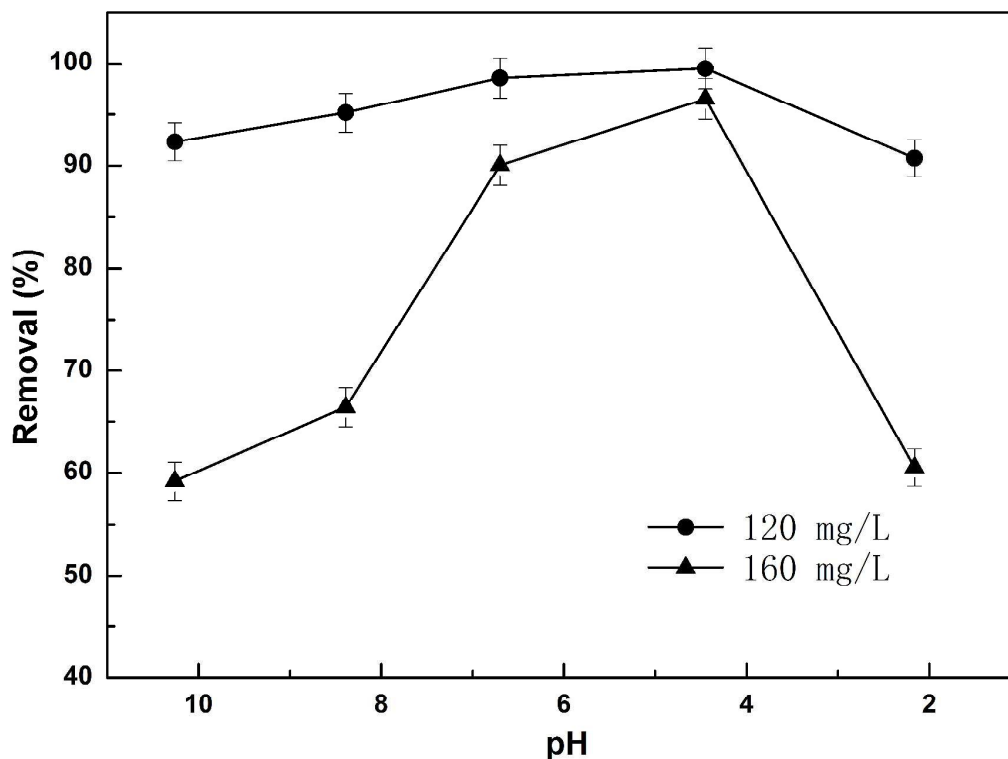


Fig. 4. Adsorption percentage of Rh6G by AC-PEI-SAA at different pH

It is known that the removal of organic matters from aqueous solutions depends on the initial solution pH since the surface charge of the adsorbent varies with the change of pH value. In addition, the solution pH also affect the degree of ionization of organic matters and concentration of the counter  $\text{H}^+$  ions of the surface group<sup>29</sup>. So, an optimum pH is important parameter during the dye adsorption process. In this study, the effect of solution pH on the adsorption of Rh6G was studied in the pH range of 2-11 with two different initial concentrations (120 mg/L and 160 mg/L). The effect of pH on the adsorption of cationic dye by the multicarboxyl adsorbent is presented in **Fig. 4**. Fig. 4 shows the removal of dye increase with decreasing solution pH from 11 to 4.45, while dramatic declines occur when solution pH is about 2. The optimum pH

for the adsorption of Rh6G is 4.45. This indicates that carboxylic groups on the surface of AC might play a significant role for adsorption of Rh6G, which is mainly achieved by electrostatic interaction between cationic dye molecules and anionic carboxylic groups<sup>30</sup>. At high acidic media (pH=2.2), hydrochloric acid lead to strong protonation and partly inhibit electrostatic interaction between negatively charged carboxylic groups and positively charged dye ions because hydrogen ion in the solution could compete with cationic dyes for active sites on the AC-PEI-SAA surface. At slightly acidic condition (pH=4.45), the carboxylic groups of AC-PEI-SAA (originated from the grafting of succinyl groups) are deprotonated and interact with the positively charged Rh6G<sup>31</sup>. At basic media (pH > 7), the carboxylic groups are partly interacted with ·OH, which results in the reduction of active sites on the functionalized AC as well as decrease of the dye uptakes. Hence, the mechanism of the adsorption process mainly involved electrostatic interaction between cationic dyes and negatively charged carboxylic groups.

### 3.3 Kinetics of adsorption

In order to further understand the characteristics of the adsorption process, including the rate controlling steps and potential mechanism of adsorption, the kinetic behavior of the adsorption process is studied under the pH =4.45 at 25°C using the initial dye concentrations of 160 mg/L . The adsorption kinetics data was evaluated using pseudo-first-order, pseudo-second-order kinetic and intraparticle equations to investigate the controlling mechanism of dye adsorption from aqueous solution. The pseudo-first-order kinetic model describes the reversibility of equilibrium between liquid and solid phases. The model assumes that adsorption is controlled by film diffusion step. The pseudo-second-order kinetic model is suitable for the reaction of the saturated sites, which indicates that the adsorption mechanism may depend on the adsorbate and adsorbent. The internal particle diffusion assumes that intraparticle diffusion is the only rate-limiting step. These three models are given as follows<sup>32-34</sup> :

The pseudo-first-order rate expression is given as:

$$\ln(q_e - q_t) = \ln q_e - k_1 t \quad (2)$$

where  $q_e$  and  $q_t$  (mg/g) are the amounts of dye adsorbed on adsorbent at equilibrium and at time  $t$ , respectively, and  $k_1$  ( $\text{min}^{-1}$ ) is the rate constant of pseudo-first-order model. Fig. 5a shows that experimental data are remarkably different from the pseudo-first-order model, the  $q_e$  value do not agree with experimental values and the fitted value  $R^2$  is also not ideal (Table 1). It implies that adsorption is not mainly controlled by film diffusion step.

The pseudo-second-order rate expression is given as:

$$\frac{t}{q_t} = \frac{1}{q_e} t + \frac{1}{k_{ad} q_e^2} \quad (3)$$

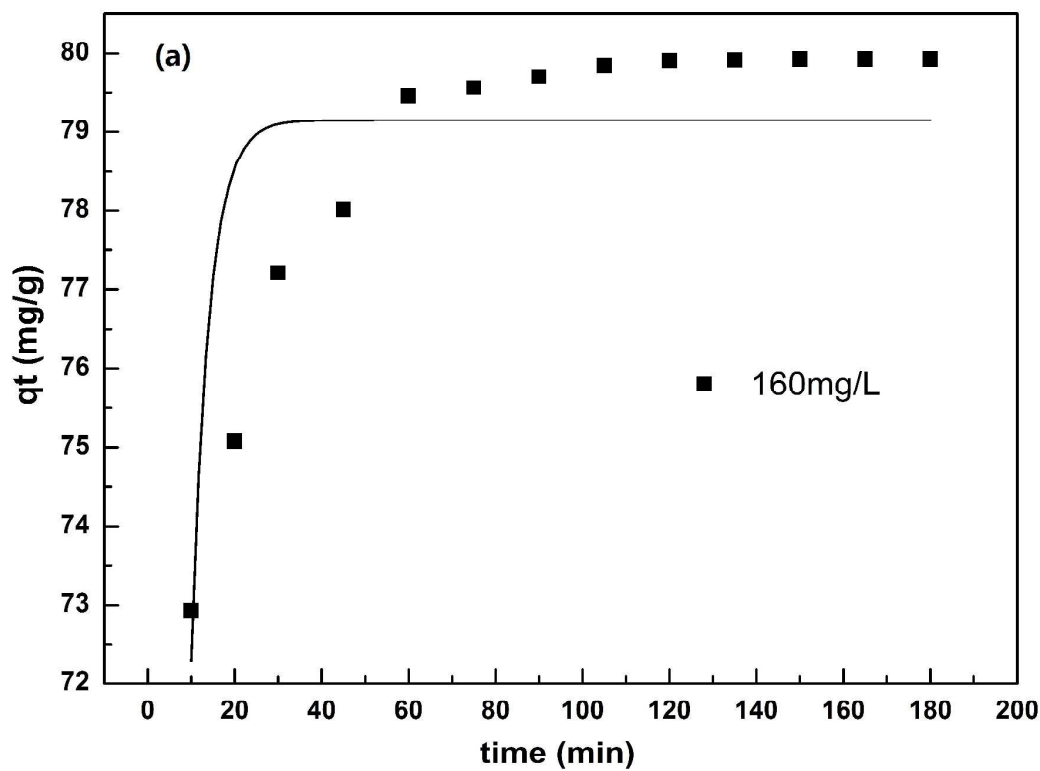
where  $k_{ad}$  ( $\text{g}/(\text{mg min})$ ) is the equilibrium rate constant of pseudo-second-order adsorption. The values of  $q_e$  and  $k_{ad}$  can be obtained from the slope and intercept of the  $t/q_t$  vs  $t$  plots and are given in Table 1. The pseudo-second-order model provides higher  $R^2$ , closer adsorption capacity compared with experimental values and excellent linearity (Fig. 5b), indicating that adsorption may be related to the electron transfer between the adsorbent and the adsorbate.

The intraparticle diffusion model is further employed to identify the involved steps during adsorption process. The rate parameter of intraparticle diffusion can be defined as:

$$q_t = k_i t^{0.5} \quad (4)$$

$k_i$  ( $\text{mg}/(\text{g min}^{0.5})$ ) is the rate constant of intraparticle diffusion which is determined from the linear plot of  $q_t$  versus  $t^{0.5}$  and is listed in Table 1. The value of  $k_i$  calculated from the slope of  $q_t$  versus  $t^{1/2}$  suggested different adsorption stages and adsorption rate. As shown in Fig. 5c, multilinearities imply more than one process during the adsorption. If the intraparticle diffusion is the only rate-controlling step, the plot passes through the origin. If not, the film diffusion controls the adsorption to some degrees<sup>35</sup>. The first portion  $k_{i1}$  describes the diffusion of cationic dyes from the solution to the exterior surface of adsorbent until the surface functional sites is occupied. This can be attributed to a favorable attraction between dye molecules and

the carboxylic groups. The second portion  $k_{12}$  is related to filling of molecular dye in the pores of AC-PEI-SAA particles, and the diffusion rate decreases with increasing the adsorption capacity until it gradually becomes gently. This suggested a gradual equilibrium due to the intraparticle diffusion of Rh6G. The third stage  $k_{13}$  reaches the final balance duo to adsorption-desorption equilibrium.



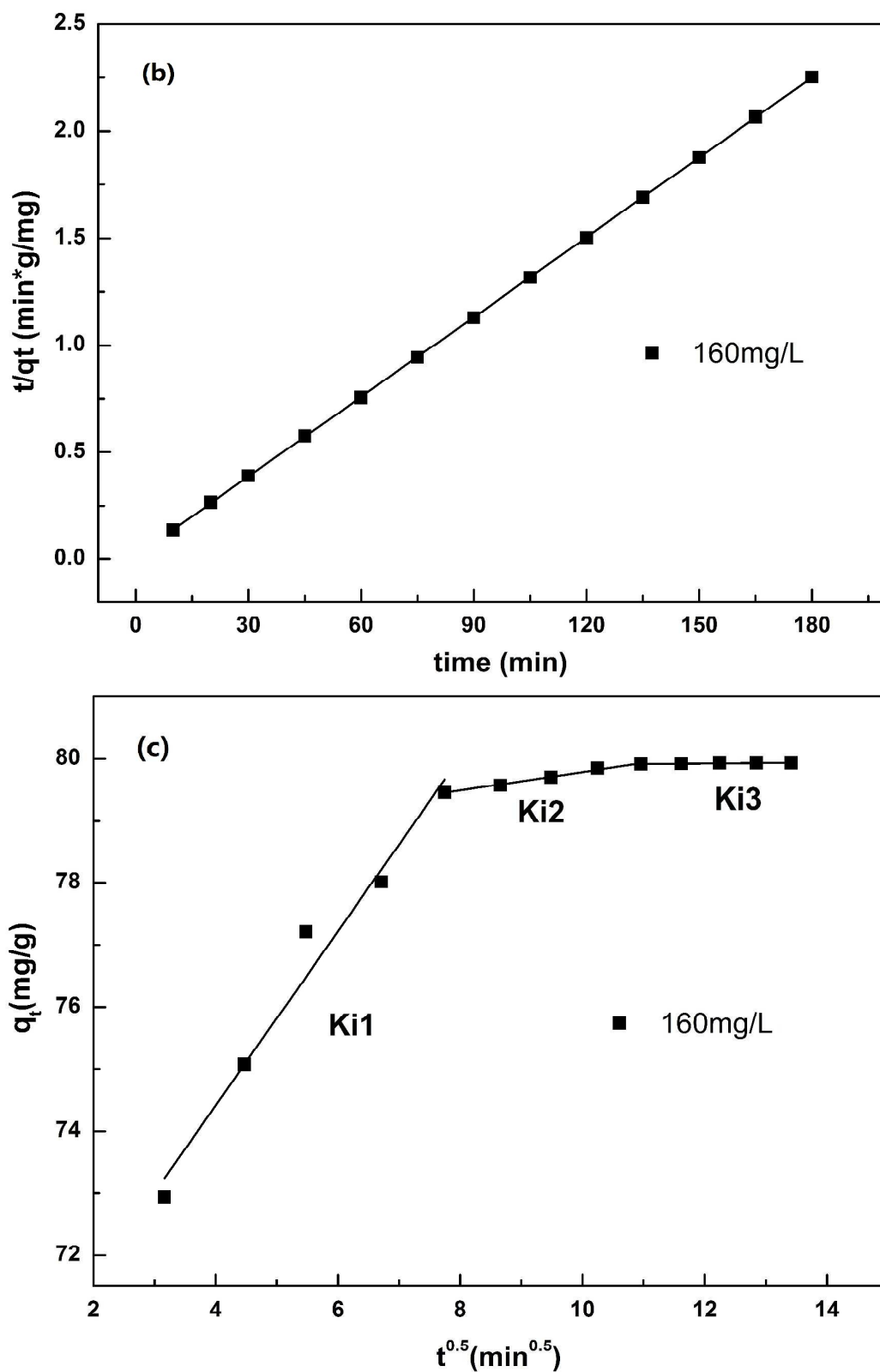


Fig 5. (a) The pseudo-second-order adsorption kinetic model of Rh6G. (b) The pseudo-first-order adsorption kinetic model of Rh6G. (c) The intraparticle rate.

Table 1. Kinetic parameters of three models for the adsorption of Rh6G on AC-PEI-SAA

Model	Parameter	Concentration
		160 mg/L
Pseudo-first order kinetic	$k$ ( $\text{min}^{-1}$ )	0.2446
	$q_e$ calculate ( $\text{mg/g}$ )	79.1469
	$R^2$	0.61009
Pseudo-second order kinetic	$k_{ad}$ ( $(\text{g/mg min})$ )	0.0111
	$q_e$ calculate ( $\text{mg/g}$ )	80.5153
	$R^2$	0.99998
Intraparticle diffusion	$k_{i1}$ ( $\text{mg}/(\text{g min}^{1/2})$ )	1.40132
	$k_{i2}$	0.14824
	$k_{i3}$	0.00836

### 3.4 Adsorption isotherms

Adsorption isotherms present the relationship between the amount of adsorbate on the solid phase and the concentration of adsorbate in solution when both phases are in equilibrium. Langmuir, Freundlich and Temkin isotherm model are employed to study adsorption behavior. The Langmuir isotherm assumes the equilibrium parameters of monolayer adsorption on homogenous surfaces by uniformly distributed adsorption sites<sup>36</sup>, which can be expressed as :

$$\frac{C_e}{q_e} = \frac{1}{bq_m} + \frac{C_e}{q_m} \quad (5)$$

where  $C_e$  ( $\text{mg/L}$ ) is the equilibrium concentration of dye,  $q_e$  ( $\text{mg/g}$ ) is the adsorption capacity at equilibrium,  $q_m$  and  $b$  are the maximum adsorption capacity ( $\text{mg/g}$ ) and the equilibrium adsorption constant ( $\text{L/mg}$ ) was calculated by the fitting curve.

While the Freundlich isotherm is derived by assuming a heterogeneous surface

with non-uniform distribution of adsorption and multilayer reversible adsorption. Freundlich isotherm can be expressed<sup>37</sup>:

$$\ln q_e = \ln k + \frac{1}{n} \ln C_e \quad (6)$$

Where the empirical constants  $k$  is the anti-logarithm of the y-intercept, indicating adsorption capacity and  $n$  is the reciprocal of the slope, indicating the adsorption intensity.

The Temkin isotherm was based on premise: the increase of coverage due to adsorbate-adsorbent interactions leads to linear decrease in heat of adsorption of all molecules in the layer. Temkin isotherm model equation can be expressed as:

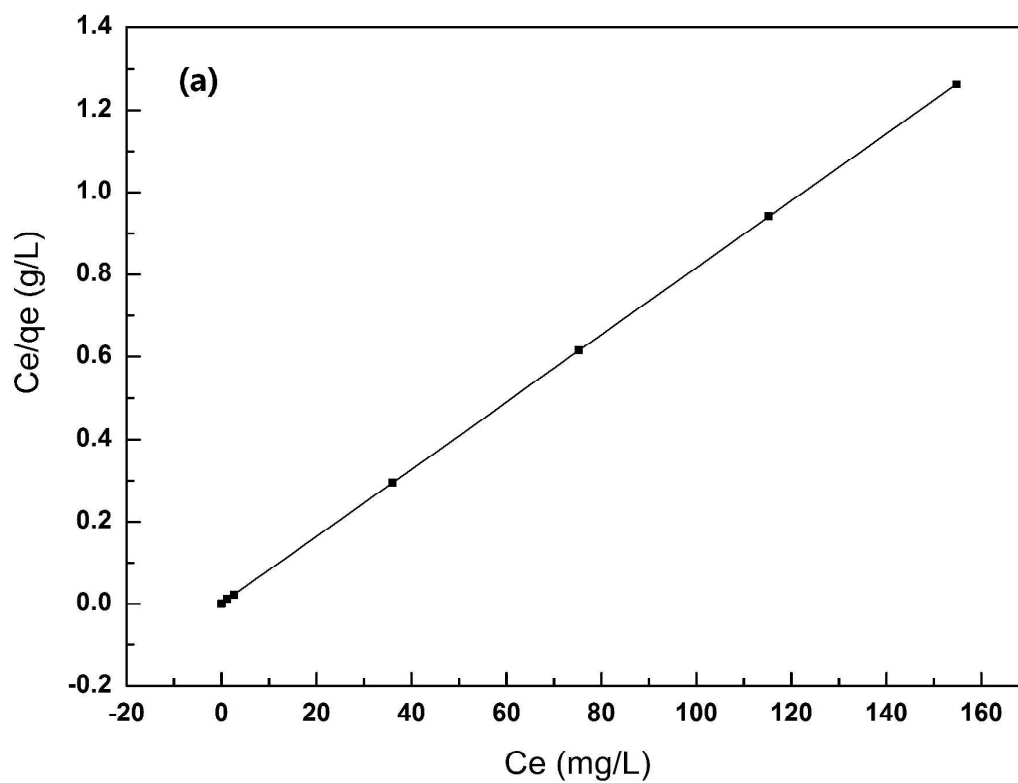
$$q_e = B_T \ln K_T + B_T \ln C_e \quad (7)$$

where  $K_T$  is the equilibrium binding constant (L/mg),  $B_T$  is related to the heat of adsorption.

The adsorption data from Langmuir, Freundlich and Temkin models are summarized in **Table 2**. The Langmuir model (**Fig.6a**) fits better than the Freundlich model (**Fig .6b**) and Temkin model (**Fig .6c**). Therefore, the adsorption of Rh6G onto AC-PEI-SAA is a monolayer adsorption. This indicates that the carboxylic groups are uniformly and entirely coated on the surface of substrate. The maximum adsorption capacities of AC, AC-COOH and AC-PEI-SAA at 25°C were about 33.18, 45.07 and 122.55 mg/g, respectively. The result showed that the grafted multicarboxyl on AC markedly improved the adsorption capacity. The monolayer adsorption capability of R6G obtained in the experiment and other results reported in literature appear in **Table 3**. It can be found that AC-PEI-SAA showed a greater adsorption capability compared to other adsorbents, including activated carbon and some other low-cost adsorbents. This indicated that AC-PEI-SAA was a promising adsorbent for the removal of Rh6G from aqueous solutions.

In order to evaluate the effect of temperature on the adsorption of dyes, 20 mg of AC-PEI-SAA were added to 10 ml of solutions containing Rh6G at the concentration of 200 mg/L. The mixtures were oscillated at 25°C, 35°C, 45°C for 2.5 h. The

experimental results showed that the residual concentrations of Rh6G were 11.44, 7.68, 5.51 mg/L, respectively. The removal ratio increased with the increase of temperature, indicating that the adsorption process of the modified activated carbon was an endothermic process. So, the increase of temperature is beneficial to adsorption.



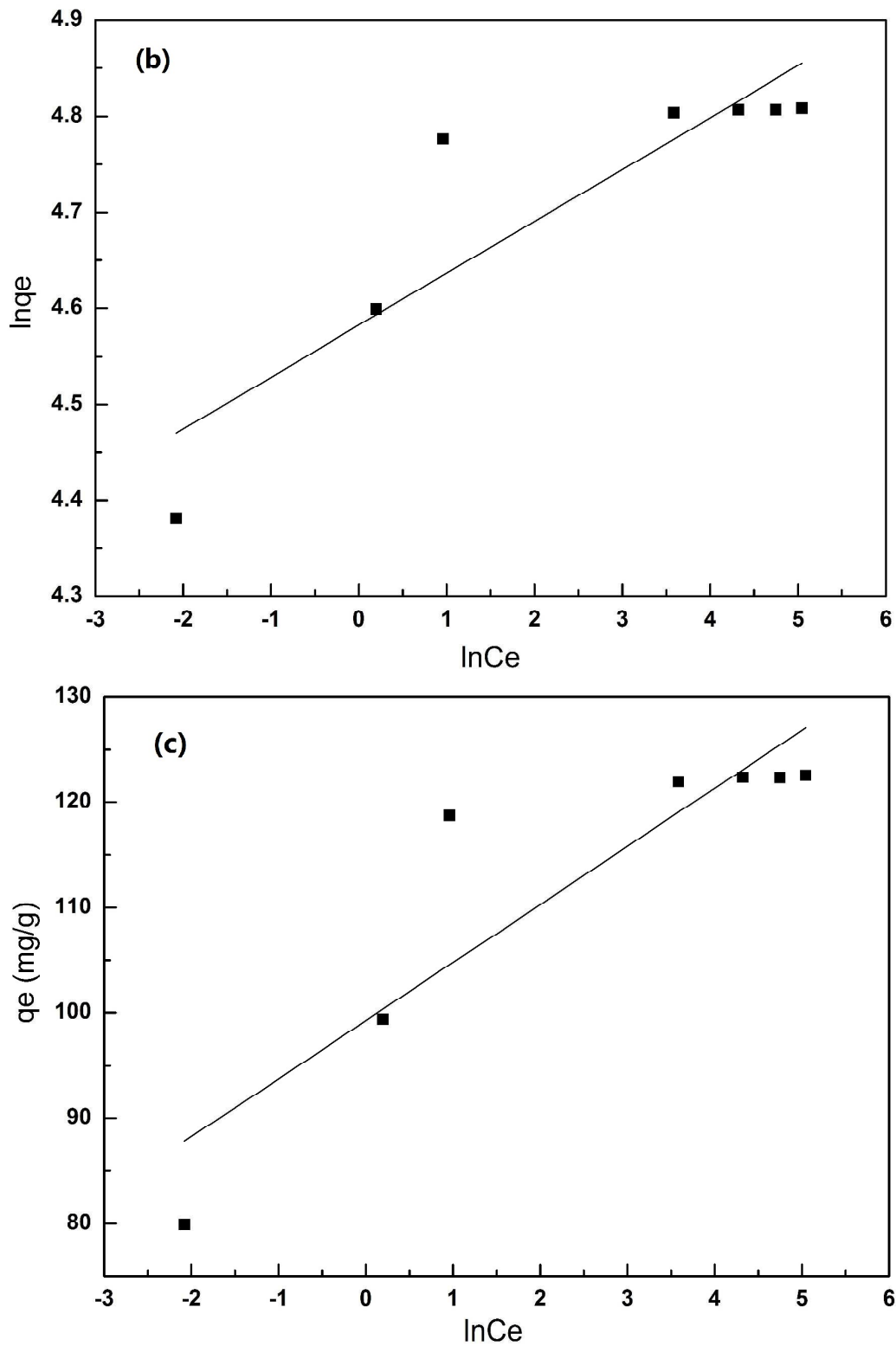


Fig. 6. (a) Langmuir model. (b) Freundlich model. (c) Temkin model.

Table 2. Isotherm parameters for the adsorption of Rh6G on AC-PEI-SAA

Model	Parameter	Parameter value
		25°C
Langmuir	qm(mg/g)	122.549
	b	7.7714
	R <sup>2</sup>	0.9998
Freundlich	1/n	0.05402
	k	97.765
	R <sup>2</sup>	0.76206
Temkin	B <sub>T</sub>	5.51582
	K <sub>T</sub> (L/mg)	6.54*10 <sup>7</sup>
	R <sup>2</sup>	0.78169

Table 3. Comparison of monolayer adsorption capacity for the removal of Rh6G from aqueous solution using multicarboxyl adsorbent with adsorbents reported in literature

Adsorbent	Dye	Adsorption capacity [mg/g]	Reference
Activated carbon	Rh6G	44.7	<sup>38</sup>
Almond shell	Rh6G	32.6	<sup>39</sup>
Hexadecyl functionalized magnetic silica nanoparticles	Rh6G	35.6	<sup>40</sup>
Chitosan-g-( <i>N</i> -vinylpyrrolidone)/montmorillonite composite	Rh6G	36.6	<sup>41</sup>
Graphene oxide	Rh6G	23.30	<sup>42</sup>
Chitosan clay nanocomposite	Rh6G	440.90	<sup>43</sup>
AC-COOH	Rh6G	45.07	This study
AC-PEI-SAA	Rh6G	122.55	This study

## 3.5 Selective adsorption

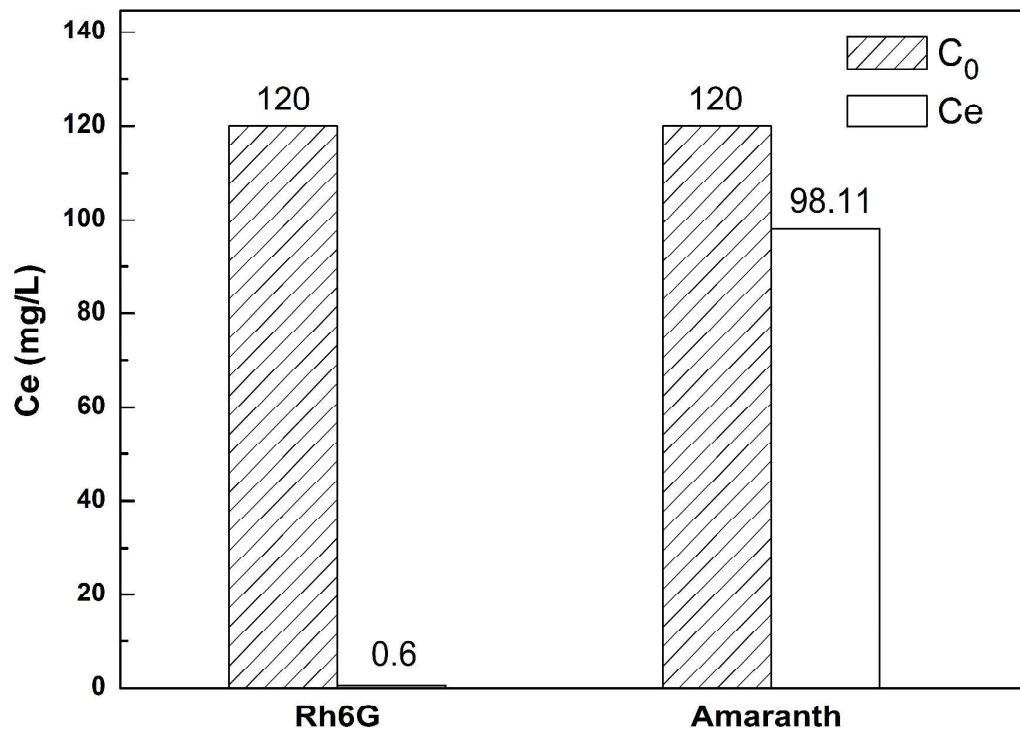


Fig 7. The selective adsorption of AC-PEI-SAA for Rh6G and Amaranth

In order to test the selective adsorption, AC-PEI-SAA is also used to absorb anionic amaranth from aqueous solutions. In a typical experiment, 20 mg of AC-PEI-SAA are dispersed into 10 ml of Amaranth at pH=4.45 with its concentration of 120 mg/L. The adsorption performance of adsorbent for R6G and Amaranth are summarized in **Fig. 7**. After 2.5h, the concentration of R6G almost decreases to zero. Conversely, the equilibrium concentration of Amaranth is about 98.11mg/L, the adsorption percent is only 18%. This indicated that the modified activated carbon selectively absorbed the cationic organics. In addition, another cationic dye (methylene blue) and two anionic dyes (alizarin red and xylenol orange) are employed to conduct adsorption experiments to further identify the universality of selective adsorption (**Fig. 8**). According to **Fig. 8**, the color of the cationic dyes almost completely disappeared due to remarkable adsorption, and the color of the three kinds of anionic dyes had no obvious change, indicating the effect of adsorption is not



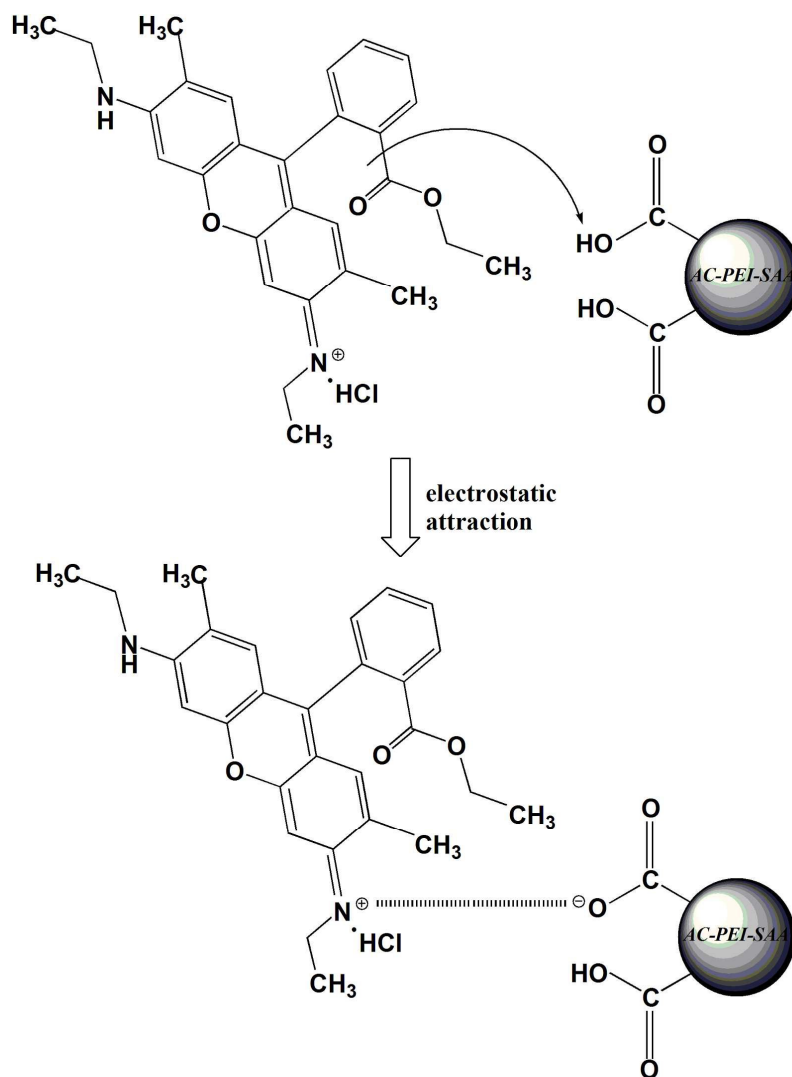


Fig. 10. Schematic illustration of the interaction between AC-PEI-SAA and Rh6G: electrostatic attraction

(surface area and pore structure) and chemical properties (surface functional groups). The specific surface area of the original AC is 1510 m<sup>2</sup>/g. The adsorption capacity of Rh6G on AC is only 33.18 mg/g. However, the specific surface area of AC-PEI-SAA is only 15.31m<sup>2</sup>/g. The adsorption capacity of Rh6G on AC-PEI-SAA is 122.55 mg/g. Therefore, we can infer that the adsorption mainly drove by surface functional groups. **Fig. 9** shows the FTIR spectra of the AC-PEI-SAA before and after adsorbed Rh6G. The two characteristic peaks of Rh6G at 3416 and 1092 cm<sup>-1</sup> are recognized in **Fig. 9b**<sup>44</sup>. **Fig. 9b** also exhibits the characteristic stretching peaks of saturated C-H (CH<sub>3</sub>) at 2932 and 2860 cm<sup>-1</sup>, stretching vibration of C=N at 2338 cm<sup>-1</sup> and the peak related to the vibration of the

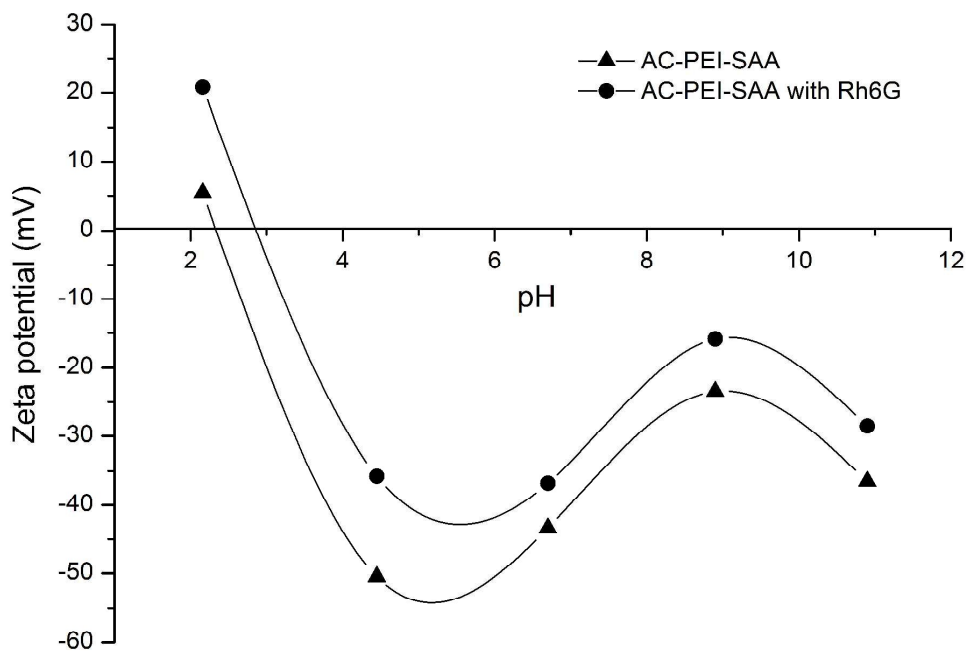


Fig. 11. The Zeta potential of AC-PEI-SAA as a function of pH at 25 °C in the absence and presence of Rh6G

aromatic ring at  $1600\text{ cm}^{-1}$  is very prominent<sup>45</sup>, which showed that the Rh6G has been anchored on the surface of adsorbent after the adsorption. It is worth nothing that the carboxyl (C=O) peak shifted to  $1719\text{ cm}^{-1}$  in Fig. 9b, due to the reaction between carboxyl functional groups and Rh6G. This can be explained by the following reason: Rh6G is a kind of cationic dye which can be adsorbed easily by electrostatic forces on negatively charged surfaces, as schematically illustrated in **Fig. 10**. Similar observation of the electrostatic attraction between of cationic dye and magnetite loaded multi-wall carbon nanotube has been reported by Jiang et al<sup>29</sup>. In order to verify the hypothesis of electrostatic adsorption, Zeta potential is applied to investigate charge type of material surface, charge quantity and its stability in different pH solutions. Zeta potential of AC-PEI-SAA and AC-PEI-SAA with Rh6G is shown in **Fig. 11**. The isoelectric point (iep) of AC-PEI-SAA is observed at pH 2.3. Above this pH, AC-PEI-SAA particles are negative in aqueous solutions and they can capture positive cationic dyes like Rh6G in theory. The Zeta potentials of AC-PEI-SAA with Rh6G are found to shift toward the positive direction. The largest increment of Zeta potential occur at pH 4.45, suggesting a large amount of Rh6G has been anchored on the AC-PEI-SAA surface by the electrostatic interaction. This is

consistent with the fact that the optimum pH is 4.45. From the above analysis, it is evident that the electrostatic interaction is the main mechanism for the dye adsorption.

#### 4. Conclusions

An activated carbon-based multicarboxyl adsorbent was prepared via grafting succinic anhydride on AC. The adsorption capacity of Rh6G onto the multicarboxyl adsorbent was much better than that of AC at pH 4.45. Adsorption kinetics followed the pseudo-second-order model. The boundary layer diffusion was the rate-controlling step. According to Langmuir model, the adsorption was localized to a monolayer and the maximum adsorption capacity of Rh6G on AC-PEI-SAA was 122.55 mg/g. The multicarboxyl groups on the surface of the adsorbent play a crucial role during adsorption process. The Zeta potential and FTIR analysis suggested that the electrostatic interaction was the primary mechanism for the dye adsorption. The multicarboxyl adsorbent selectively removes the cationic dyes from aqueous solution. Above all, the activated carbon-based multicarboxyl adsorbent has the potential to remove cationic dyes for water treatment.

#### Acknowledgements

This work was supported by the National Science Foundation of China (No. 51464024), and Young and Middle-aged Academic Technology Leader Backup Talent Cultivation Program in Yunnan Province (2012HB008).

#### References

1. G. Crini, *Bioresource Technology*, 2006, **97**, 1061-1085.
2. F. Fu and Q. Wang, *Journal of Environmental Management*, 2011, **92**, 407-418.
3. H. Zollinger, New York: John Wiley-VCH Publishers, Editon edn., 2002.
4. C. I. Pearce, J. R. Lloyd and J. T. Guthrie, *Dyes and Pigments*, 2003, **58**, 179-196.
5. P. C. C. Faria, J. J. M. Órfão and M. F. R. Pereira, *Water Research*, 2004, **38**, 2043-2052.
6. F. P. van der Zee and S. Villaverde, *Water Research*, 2005, **39**, 1425-1440.
7. M. Rafatullah, O. Sulaiman, R. Hashim and A. Ahmad, *Journal of Hazardous Materials*, 2010, **177**, 70-80.
8. N. Daneshvar, M. Ayazloo, A. R. Khataee and M. Pourhassan, *Bioresource Technology*, 2007, **98**, 1176-1182.
9. M. Riera-Torres, C. Gutiérrez-Bouzán and M. Crespi, *Desalination*, 2010, **252**, 53-59.

10. T.-H. Kim, C. Park, J. Yang and S. Kim, *Journal of Hazardous Materials*, 2004, **112**, 95-103.
11. Y. He, G. Li, H. Wang, J. Zhao, H. Su and Q. Huang, *Journal of Membrane Science*, 2008, **321**, 183-189.
12. J. Labanda, J. Sabaté and J. Llorens, *Chemical Engineering Journal*, 2011, **166**, 536-543.
13. Y. Dong, H. Lin and F. Qu, *Chemical Engineering Journal*, 2012, **193-194**, 169-177.
14. J. Galán, A. Rodríguez, J. M. Gómez, S. J. Allen and G. M. Walker, *Chemical Engineering Journal*, 2013, **219**, 62-68.
15. G.-P. Hao, W.-C. Li, S. Wang, S. Zhang and A.-H. Lu, *Carbon*, 2010, **48**, 3330-3339.
16. C. Moreno-Castilla, *Carbon*, 2004, **42**, 83-94.
17. M. Ghaedi, F. Ahmadi, Z. Tavakoli, M. Montazerzohori, A. Khanmohammadi and M. Soylak, *Journal of Hazardous Materials*, 2008, **152**, 1248-1255.
18. H. Choi, W. Jung, J. Cho, B. Ryu, J. Yang and K. Baek, *J. Hazard. Mater.*, 2009, **166**, 642-646.
19. M. Auta and B. H. Hameed, *Colloids and Surfaces B: Biointerfaces*, 2013, **105**, 199-206.
20. G. M. Nabil, N. M. El-Mallah and M. E. Mahmoud, *Journal of Industrial and Engineering Chemistry*, 2014, **20**, 994-1002.
21. S. Greg and K. Sing, *New York*, 1982.
22. S. Largergren, *Handlingar*, 1898, **24**, 1-39.
23. A.-N. A. El-Hendawy, *Carbon*, 2003, **41**, 713-722.
24. R. M. Silverstein, F. X. Webster, D. Kiemle and D. L. Bryce, *Spectrometric identification of organic compounds*, John Wiley & Sons, 2014.
25. J. A. Syed, H. Lu, S. Tang and X. Meng, *Applied Surface Science*, 2015, **325**, 160-169.
26. D. Şen Karaman, T. Gulin-Sarfraz, G. Hedström, A. Duchanoy, P. Eklund and J. M. Rosenholm, *Journal of Colloid and Interface Science*, 2014, **418**, 300-310.
27. T. Yoshimura, K. Matsuo and R. Fujioka, *Journal of Applied Polymer Science*, 2006, **99**, 3251-3256.
28. W. Y. Li, A. X. Jin, C. F. Liu, R. C. Sun, A. P. Zhang and J. F. Kennedy, *Carbohydrate Polymers*, 2009, **78**, 389-395.
29. L. Ai, C. Zhang, F. Liao, Y. Wang, M. Li, L. Meng and J. Jiang, *Journal of Hazardous Materials*, 2011, **198**, 282-290.
30. Y. Zhou, M. Zhang, X. Hu, X. Wang, J. Niu and T. Ma, *Journal of Chemical & Engineering Data*, 2013, **58**, 413-421.
31. G. Z. Kyzas, P. I. Sifaka, E. G. Pavlidou, K. J. Chrissafis and D. N. Bikiaris, *Chemical Engineering Journal*, 2015, **259**, 438-448.
32. Y. Zhao, Z. Xue, X. Wang, L. Wang and A. Wang, *J. Wuhan Univ. Technol.-Mat. Sci. Edit.*, 2012, **27**, 931-938.
33. Y. S. Ho and G. McKay, *Chemical Engineering Journal*, 1998, **70**, 115-124.
34. M. Ghaedi and S. N. Kokhdan, *Desalination and Water Treatment*, 2012, **49**, 317-325.
35. Q. Qin, J. Ma and K. Liu, *Journal of Hazardous Materials*, 2009, **162**, 133-139.
36. E. Repo, J. K. Warchol, T. A. Kurniawan and M. E. T. Sillanpää, *Chemical Engineering Journal*, 2010, **161**, 73-82.
37. R. J. Umpleby Ii, S. C. Baxter, M. Bode, J. K. Berch Jr, R. N. Shah and K. D. Shimizu, *Analytica Chimica Acta*, 2001, **435**, 35-42.
38. G. Annadurai, R.-S. Juang and D.-J. Lee, *Journal of Environmental Science and Health, Part*

- A*, 2001, **36**, 715-725.
39. H. B. Senturk, D. Ozdes and C. Duran, *Desalination*, 2010, **252**, 81-87.
40. Y.-P. Chang, C.-L. Ren, Q. Yang, Z.-Y. Zhang, L.-J. Dong, X.-G. Chen and D.-S. Xue, *Applied Surface Science*, 2011, **257**, 8610-8616.
41. A. Vanamudan, K. Bandwala and P. Pamidimukkala, *International Journal of Biological Macromolecules*, 2014, **69**, 506-513.
42. H. Ren, D. D. Kulkarni, R. Kodiyath, W. Xu, I. Choi and V. V. Tsukruk, *ACS applied materials & interfaces*, 2014, **6**, 2459-2470.
43. A. Vanamudan and P. Pamidimukkala, *International Journal of Biological Macromolecules*, 2015, **74**, 127-135.
44. S. Bakkialakshmi and T. menaka, *Spectrochimica Acta Part A: Molecular and Biomolecular Spectroscopy*, 2011, **81**, 8-13.
45. A. S. Al Dwayyan, S. M. H. Qaid, M. A. Majeed Khan and M. S. Al Salhi, *Optical Materials*, 2012, **34**, 761-768.